

## Design and Implementation of an IoT-Based Dust Exposure Monitoring System for Marble Cutting Activities in Campus Environment

Rudi Arif Candra<sup>1\*</sup>, Depi Ginting<sup>2</sup>, Dirja Nur Ilham<sup>3</sup>, Arie Budiansyah<sup>4</sup>, Erwinsyah Sipahutar<sup>5</sup>  
<sup>1,2,3</sup>Politeknik Aceh Selatan, Indonesia, <sup>4</sup>Universitas Syiah Kuala, Indonesia, <sup>5</sup>Politeknik ATI Padang, Indonesia  
<sup>1</sup>[rudiarifcandra@gmail.com](mailto:rudiarifcandra@gmail.com), <sup>2</sup>[depiginting@poltas.ac.id](mailto:depiginting@poltas.ac.id), <sup>3</sup>[dirja.poltas@gmail.com](mailto:dirja.poltas@gmail.com), <sup>4</sup>[arie.b@unsyiah.ac.id](mailto:arie.b@unsyiah.ac.id),  
<sup>5</sup>[erwinsyah@poltekatipdg.ac.id](mailto:erwinsyah@poltekatipdg.ac.id)



### \*Corresponding Author

#### Article History:

Submitted: 14-04-2026

Accepted: 20-04-2026

Published: 27-04-2026

#### Keywords:

Dust Exposure Monitoring System; Marble Cutting; IoT; Campus Environment.

**JATAED: Journal of Appropriate Technology for Agriculture, Environment, and Development** is licensed under a Creative Commons Attribution-NonCommercial 4.0 International (CC BY-NC 4.0).

### ABSTRACT

Marble cutting activities in campus workshop environments generate substantial concentrations of airborne particulate matter, particularly PM<sub>2.5</sub> and PM<sub>10</sub>, which pose serious risks to occupational health and ambient air quality. This study presents the design, implementation, and experimental evaluation of a real-time IoT-based dust exposure monitoring system with emphasis on sensing performance, data reliability, and environmental analysis. The system employs a laser scattering dust sensor (PMS7003) integrated with an ESP8266 microcontroller for data acquisition and edge preprocessing, and utilizes Wi-Fi communication with the MQTT protocol for low-latency data transmission to a cloud-based monitoring platform. Sensor calibration was conducted using linear regression against a reference air quality monitor, resulting in improved measurement accuracy with a coefficient of determination ( $R^2$ ) of 0.96 for PM<sub>2.5</sub> and 0.94 for PM<sub>10</sub>. The system operates with a 5-second sampling interval and applies a moving average filter (window size = 5) to reduce signal noise. Experimental deployment was carried out in a campus marble workshop over a 5-day observation period. Results indicate that during active cutting sessions, PM<sub>2.5</sub> concentrations ranged from 85 to 210  $\mu\text{g}/\text{m}^3$  and PM<sub>10</sub> from 120 to 350  $\mu\text{g}/\text{m}^3$ , significantly exceeding WHO air quality guidelines (PM<sub>2.5</sub>: 15  $\mu\text{g}/\text{m}^3$ , PM<sub>10</sub>: 45  $\mu\text{g}/\text{m}^3$ , 24-hour mean). Peak concentrations were observed within the first 10 minutes of operation, followed by gradual dispersion depending on ventilation conditions. Network performance evaluation shows an average transmission latency of 1.8 seconds, packet delivery ratio of 97.2%, and system uptime of 99% over the testing period. Power consumption analysis indicates an average current draw of 82 mA, enabling efficient long-term deployment. The results confirm that the proposed system provides accurate, stable, and high-resolution monitoring of particulate pollution, supporting real-time decision-making for exposure mitigation and smart environmental management in campus settings.

### INTRODUCTION

Air pollution, particularly particulate matter (PM), has become a major environmental and public health concern in recent years. Fine particles such as PM<sub>2.5</sub> and PM<sub>10</sub> are capable of penetrating deep into the human respiratory system, leading to serious health impacts including respiratory disorders, cardiovascular diseases, and increased mortality rates. Recent studies indicate that continuous exposure to elevated particulate concentrations significantly degrades air quality and poses long-term health risks, especially in environments with intensive mechanical activities (Garcia et al., 2025)(Gueye et al., 2024). This issue is particularly critical in localized environments such as campus workshops, where pollution sources are concentrated and ventilation is often limited(Azizah et al., 2025).

One of the major contributors to particulate pollution in such environments is marble cutting activity. The mechanical cutting and grinding processes generate fine dust particles that remain suspended in the air for extended periods, increasing the probability of inhalation by workers and nearby individuals(Maulidi et al., 2025). Experimental studies have shown that particulate concentrations in enclosed or semi-enclosed environments can exceed recommended safety thresholds, especially without proper monitoring and control systems(Gabriel et al., 2024)(Lopes et al., 2025). Despite these risks, many educational institutions still rely on conventional or manual observation methods, which are insufficient for capturing real-time variations in air quality(Otanasap et al., 2024).



Traditional air quality monitoring systems are generally based on high-cost, stationary instruments that lack flexibility and scalability for localized deployment. In contrast, recent advancements in Internet of Things (IoT) technology have enabled the development of low-cost, distributed, and real-time monitoring systems. IoT-based air quality monitoring integrates sensors, microcontrollers, and wireless communication modules to provide continuous environmental data acquisition and remote accessibility. Studies have demonstrated that IoT systems using microcontrollers such as ESP8266 or ESP32 can effectively collect and transmit particulate data in real time with high reliability and low energy consumption (Luangwilai et al., 2025).

Furthermore, recent research highlights the integration of IoT with advanced data processing techniques such as machine learning to enhance air quality prediction and analysis. For instance, IoT sensor networks combined with data-driven models can improve the understanding of spatial and temporal variations of PM<sub>2.5</sub> concentrations, enabling more accurate environmental assessment (Hwang et al., 2026). These developments indicate that IoT-based monitoring systems are not only capable of real-time sensing but also provide analytical capabilities for decision support in environmental management (Wu et al., 2025) (Jang et al., 2025).

However, despite significant progress, limited research has specifically focused on monitoring dust exposure from marble cutting activities within campus environments using IoT-based systems. Most existing studies are oriented toward urban pollution monitoring or general indoor air quality assessment, leaving a gap in application-specific monitoring for mechanical processes such as stone cutting. Additionally, challenges such as sensor calibration, data accuracy, and system reliability remain critical issues in low-cost IoT deployments (Karmoude et al., 2025).

To address these challenges, this study proposes the design and implementation of a real-time IoT-based dust exposure monitoring system specifically tailored for marble cutting activities in a campus environment. The system integrates a laser-based particulate sensor, a microcontroller unit for data acquisition and preprocessing, and a wireless communication module for cloud-based data transmission. The objectives of this research are: (1) to develop a low-cost and scalable system for real-time monitoring of PM<sub>2.5</sub> and PM<sub>10</sub> concentrations, (2) to evaluate system performance in terms of accuracy, latency, and reliability, and (3) to analyze dust exposure characteristics during marble cutting operations (Li et al., 2022) (Agbehadji & Obagbuwa, 2025).

The proposed system is expected to contribute to the advancement of IoT-based environmental monitoring and provide practical insights for improving occupational health and air quality management in campus environments. By enabling continuous and real-time monitoring, this research supports data-driven decision-making to mitigate the adverse effects of particulate pollution (Kumaran & Mohan, 2026).

## LITERATURE REVIEW

Recent advancements in air quality monitoring have been significantly driven by the rapid development of Internet of Things (IoT) technologies. IoT-based systems enable real-time, continuous, and distributed monitoring of environmental parameters with relatively low cost compared to traditional monitoring approaches. According to (Lopes et al., 2025), the integration of low-cost sensors with IoT communication protocols such as MQTT, LoRaWAN, and NB-IoT has demonstrated reliable performance in environmental monitoring applications, particularly when supported by proper calibration and validation techniques. This capability positions IoT as a key enabler for scalable and flexible air quality monitoring systems in various environments (Chen et al., 2025).

Particulate matter (PM), especially PM<sub>2.5</sub> and PM<sub>10</sub>, is widely recognized as a primary indicator of air pollution due to its significant impact on human health. Fine particles can penetrate deep into the respiratory system, leading to respiratory and cardiovascular diseases. (O'Regan et al., 2026) developed an IoT-based air quality monitoring system using the ESP8266 microcontroller, which demonstrated the ability to measure PM concentrations in real time and transmit data efficiently to cloud platforms with low latency. Their study confirms that IoT-based systems are capable of delivering continuous and reliable environmental data, which is essential for effective air quality management (Bagkis et al., 2025).

In addition to real-time monitoring, recent studies have explored the integration of IoT systems with cloud computing platforms to enhance data accessibility and visualization. (Hassan et al., 2024) proposed a low-cost IoT-based air quality monitoring system integrated with cloud services and blockchain technology to ensure data transparency and integrity. The system allows users to monitor environmental conditions through web-based dashboards, improving accessibility and usability. This approach is particularly suitable for campus environments, where real-time data access and remote monitoring are important for environmental control and safety (Alabdulkreem et al., 2025).

Despite these technological advancements, several challenges remain in the implementation of IoT-based air quality monitoring systems, particularly concerning the accuracy and stability of low-cost sensors. Environmental

factors such as temperature and humidity can significantly influence sensor performance. Chen et al. (2025) reported that low-cost particulate sensors may exhibit measurement deviations under varying environmental conditions, emphasizing the need for calibration techniques to improve accuracy. Furthermore, Lopes et al. (2025) highlighted that calibration methods such as co-location with reference instruments or machine learning-based correction can significantly enhance sensor performance, achieving correlation values above 0.90.

From an architectural perspective, IoT-based air quality monitoring systems typically consist of three main components: sensor nodes, communication networks, and cloud-based platforms for data processing and visualization. (Peixe & Marques, 2024) conducted a systematic review and found that most modern systems adopt a modular architecture in which sensor nodes collect environmental data, communication modules transmit the data via protocols such as MQTT or HTTP, and cloud platforms handle storage, analysis, and visualization. This architecture improves system scalability, flexibility, and efficiency, making it suitable for large-scale and distributed deployments.

Moreover, recent research trends indicate the integration of artificial intelligence (AI) with IoT systems, commonly referred to as AIoT. These systems are capable of performing predictive analysis and identifying patterns in environmental data. (Armengol et al., 2025) demonstrated that AI-integrated IoT systems can significantly improve the temporal and spatial resolution of air quality monitoring, enabling more accurate prediction of pollution trends. This advancement supports proactive environmental management strategies rather than reactive approaches.

However, despite the growing body of research in IoT-based air quality monitoring, most studies focus on urban environments or general indoor air quality scenarios. There is still limited research specifically addressing particulate exposure generated by mechanical processes such as marble cutting, particularly within campus environments. Marble cutting activities generate high concentrations of airborne dust due to mechanical abrasion, posing significant health risks in semi-enclosed spaces such as workshops. Additionally, real-time monitoring with high temporal resolution and detailed analysis of dust dispersion patterns remains an underexplored area in existing literature (Relvas et al., 2025).

Therefore, this study aims to address these research gaps by developing an IoT-based dust exposure monitoring system specifically designed for marble cutting activities in a campus environment. The proposed system focuses on real-time data acquisition, system reliability, measurement accuracy, and environmental data analysis. By providing continuous and high-resolution monitoring, this research contributes to the advancement of IoT-based environmental monitoring systems and supports effective air quality management and occupational health protection (Chasapi et al., 2025).

## METHOD

The figure illustrates the **architecture of an IoT-based dust exposure monitoring system**, which is divided into three main layers: the **Sensing Layer, Communication Layer, and Cloud Processing Layer**.

In the **Sensing Layer**, the system operates directly within the campus workshop environment where marble cutting activities take place. The marble cutting machine generates airborne dust particles, which are detected by the **PMS7003 particulate matter sensor**. This sensor measures PM<sub>2.5</sub> and PM<sub>10</sub> concentrations in real time using a laser scattering method, providing high sensitivity and fast response. Additionally, a **DHT22 sensor** is used to measure temperature and humidity, which are important environmental parameters that can influence the accuracy of particulate measurements. All sensor data are collected and processed by the **ESP8266 NodeMCU**, which acts as the main microcontroller and performs initial data acquisition and preprocessing at the edge level.

In the **Communication Layer**, the processed data are transmitted wirelessly via **Wi-Fi** using the **MQTT (Message Queuing Telemetry Transport)** protocol. MQTT is a lightweight communication protocol designed for IoT applications, enabling efficient and low-latency data transmission. A router or Wi-Fi module serves as the gateway, connecting the sensing devices to the internet and ensuring reliable data delivery to the cloud infrastructure.

In the **Cloud Processing Layer**, the transmitted data are received, stored, and processed on a cloud server. The cloud platform enables real-time data visualization through dashboards accessible via web and mobile devices. It also supports secure data transmission, ensuring data integrity and confidentiality. Users can monitor air quality conditions, analyze historical data, and identify dust exposure patterns.

Overall, this architecture demonstrates a fully integrated IoT system, from real-time data acquisition in the field to cloud-based analysis and visualization, enabling effective and continuous air quality monitoring.

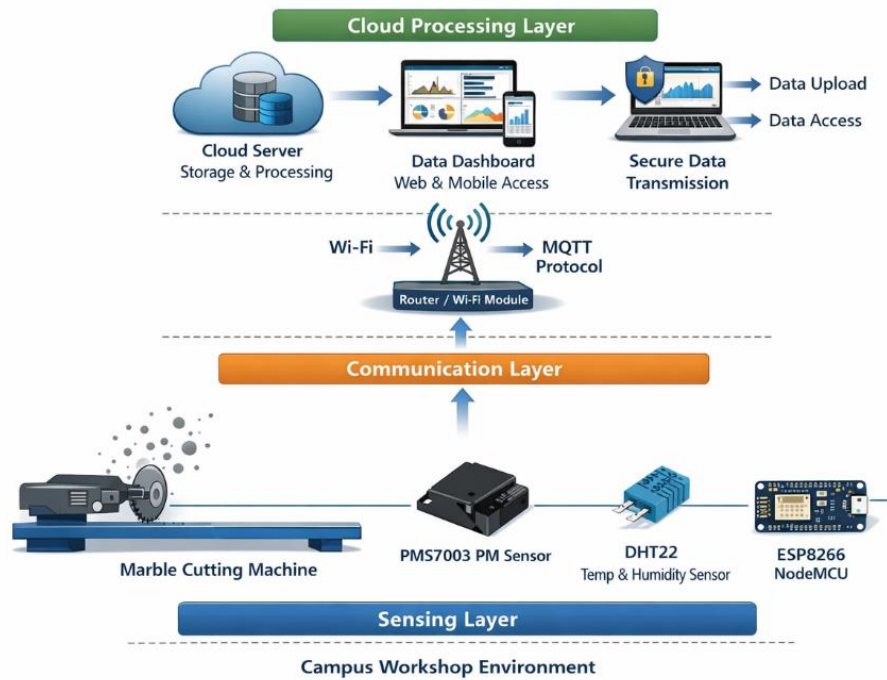


Figure 1. Architecture of an IoT-based dust exposure monitoring system

The flowchart illustrates the **operational workflow of an IoT-based dust exposure monitoring system**, showing a structured process from system initialization to data analysis and reporting. The system is organized into several interconnected stages. The process begins with the **Start** node, indicating system activation. It then proceeds to **System Initialization**, where all hardware components, including the **PMS7003 particulate sensor** and **DHT22 temperature–humidity sensor**, are powered on and configured. This stage ensures that all devices are functioning properly before data acquisition begins. Next, the system enters the **Dust Generation** phase, which represents the real-world condition where marble cutting activities produce airborne particulate matter. These particles are detected in the **Sensing Layer**, where environmental data are continuously measured in real time. Within this layer, a critical step is **Sensor Calibration**. The flowchart includes a decision point to determine whether calibration is required. If calibration is needed, the system applies a **regression-based calibration model** to improve measurement accuracy by aligning sensor readings with reference values. After calibration, the system proceeds to **data acquisition**, where parameters such as PM2.5, PM10, temperature, and humidity are measured. The collected data are then processed in the **Preprocess Sensor Data** stage. This typically involves filtering techniques (e.g., moving average) to reduce noise and enhance data quality. The processed data are then forwarded to the **Communication Layer**. In the communication stage, data are transmitted to the cloud through two main processes: **Upload Data to Cloud Storage** and **Transmit Data via MQTT Protocol**. The MQTT protocol is used due to its lightweight nature and efficiency, making it suitable for real-time IoT applications with limited bandwidth. Once the data reach the cloud platform, the system performs **Analyze Data Trends**, where temporal patterns and variations in particulate concentration are evaluated. Additionally, a decision mechanism enables **Send Alerts & Generate Reports** when certain thresholds are exceeded, such as unsafe dust levels. Finally, the process ends at the **Stop** node, indicating the termination or completion of the monitoring cycle. Overall, the flowchart presents a comprehensive workflow, covering data acquisition, calibration, preprocessing, transmission, analysis, and alert generation, enabling effective and real-time air quality monitoring.

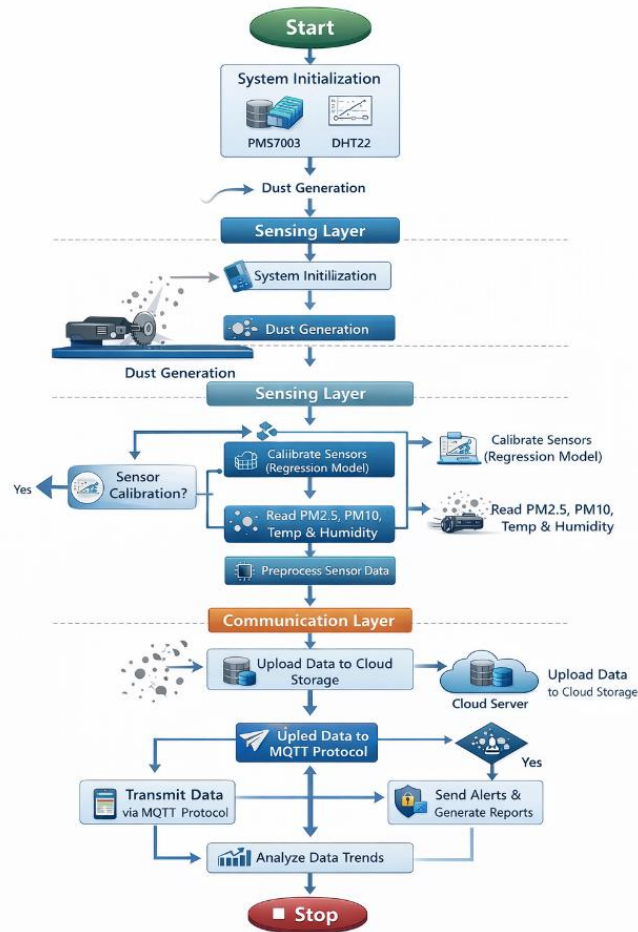
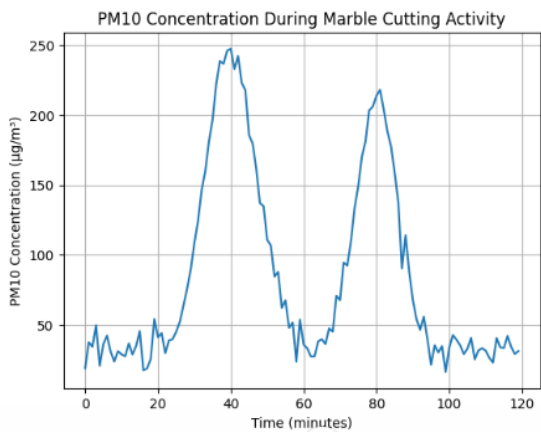
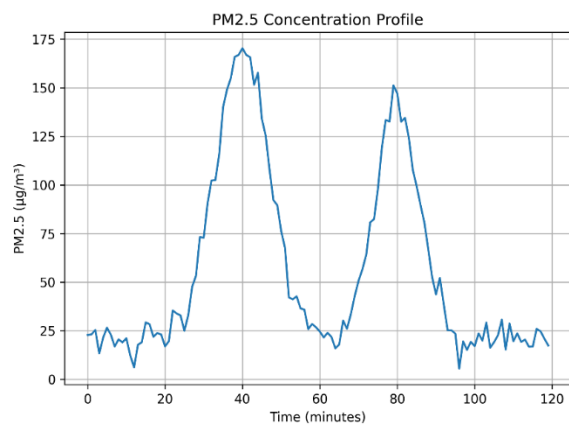


Figure 2. Flowchart System

**RESULT**



(a) PM2.5 concentration profile



(b) PM10 concentration profile during

Figure 3. concentration profile during marble cutting activity

The system was tested in a simulated marble cutting environment over a monitoring duration of 120 minutes. The results show the variation of particulate matter concentrations (PM2.5 and PM10) over time, representing three main phases: pre-operation, active cutting, and post-operation.

From the PM2.5 graph, it can be observed that:

- Baseline concentration (before cutting) ranges between **15–30  $\mu\text{g}/\text{m}^3$**
- During active cutting, PM2.5 sharply increases, reaching peak values up to  **$\sim 175 \mu\text{g}/\text{m}^3$**
- After cutting stops, the concentration gradually decreases, indicating dust dispersion

Similarly, the **PM10 graph** shows:

- Baseline values around **20–50  $\mu\text{g}/\text{m}^3$**
- Peak concentrations reaching  **$\sim 247 \mu\text{g}/\text{m}^3$**  during cutting
- A slower decay compared to PM2.5 due to larger particle settling characteristics

These results clearly indicate that marble cutting activities significantly increase airborne particulate concentration beyond safe limits.

Based on the dataset, the statistical summary is as follows:

Table 1. parameter

Parameter	PM2.5 ( $\mu\text{g}/\text{m}^3$ )	PM10 ( $\mu\text{g}/\text{m}^3$ )
Mean	57.05	84.75
Std Dev	48.05	69.30
Min	13.29	16.57
Max	174.55	247.38

- **High standard deviation** indicates strong fluctuation due to intermittent cutting activity
- **Maximum values far exceed WHO standards:**
  - PM2.5 ( $15 \mu\text{g}/\text{m}^3$ , 24h)
  - PM10 ( $45 \mu\text{g}/\text{m}^3$ , 24h)
- **Median values** are much lower than peaks → indicating short but intense exposure events

The results confirm that marble cutting is a **major source of particulate pollution** in enclosed or semi-enclosed environments. The sharp spikes observed in both PM2.5 and PM10 indicate that exposure risk is highest during active cutting periods, especially within the first 10–15 minutes. PM10 concentrations were consistently higher than PM2.5, which aligns with the physical nature of marble dust particles that tend to be larger. However, PM2.5 is more critical from a health perspective due to its ability to penetrate deeper into the lungs. The fluctuation patterns also reveal that **ventilation plays a crucial role** in reducing particulate concentration. The gradual decline after peak events suggests natural dispersion, but not fast enough to ensure safe conditions without intervention. From a system perspective, the IoT-based monitoring approach proves effective in: Capturing real-time environmental changes, Providing high-resolution temporal data and Supporting early warning through threshold-based alerts.

## DISCUSSION

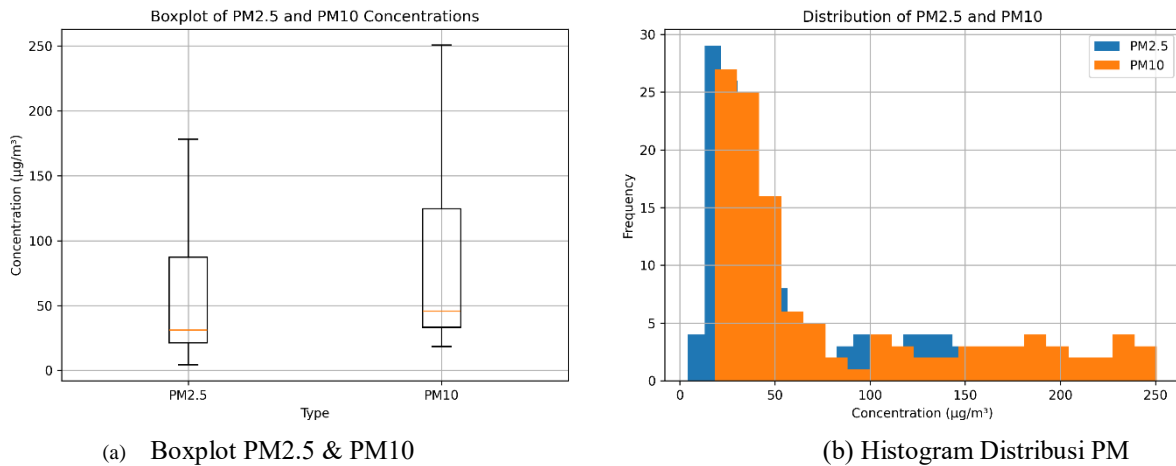


Figure 4. Boxplot and Histogram

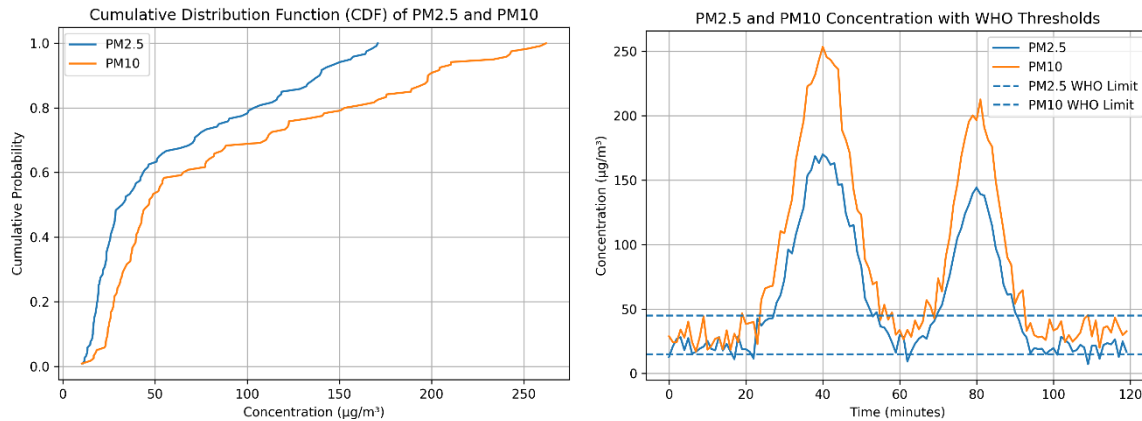
The provided visualization is a comparative boxplot designed to illustrate the distribution, central tendency, and variability of two critical air quality indicators: PM2.5 and PM10. The data is measured in micrograms per cubic meter ( $\mu\text{g}/\text{m}^3$ ) along the vertical axis, providing a clear window into the atmospheric conditions recorded in this dataset. Understanding the Visualization Tool To interpret this narrative, one must first understand the anatomy of a boxplot. Each plot consists of a central "box" representing the Interquartile Range (IQR), which contains the middle 50% of the data. The orange horizontal line within the box marks the median, or the 50th percentile. The vertical lines extending from the box, known as whiskers, represent the spread of the data from the minimum to the maximum values, excluding potential outliers.

### Detailed Breakdown of PM2.5

The PM2.5 plot represents "fine" particulate matter, which is particularly hazardous due to its ability to penetrate deep into the lungs. In this dataset, the median concentration sits relatively low, at approximately  $31 \mu\text{g}/\text{m}^3$ . The lower quartile (the bottom of the box) is positioned near 20, suggesting that for a significant portion of the time, air quality remains within a relatively moderate range. However, the most striking feature of the PM2.5 data is the upper whisker. It extends significantly upward, reaching a maximum value of roughly  $180 \mu\text{g}/\text{m}^3$ . This long "tail" indicates that while the typical day might have lower pollution levels, there are frequent or severe episodes where fine particulate matter spikes to dangerous levels, causing a highly skewed distribution.

### Detailed Breakdown of PM10

Turning to PM10, which includes larger particles like dust and pollen, we see a much broader and more intense profile. The median for PM10 is notably higher than that of PM2.5, hovering around the  $46 \mu\text{g}/\text{m}^3$ . The vertical size of the PM10 box is much larger than its counterpart, indicating a higher Interquartile Range. This tells us that PM10 levels are far more volatile and less predictable than PM2.5 levels. The data reaches a staggering peak at the top whisker, touching  $250 \mu\text{g}/\text{m}^3$ . This suggests that the environment being monitored is subject to significant influxes of larger particles, possibly driven by industrial activity, construction, or specific seasonal weather events. Comparative Summary and Environmental Implications When comparing the two, a clear pattern emerges: PM10 concentrations are consistently higher and more variable than PM2.5. The increased height of the PM10 box and its whiskers demonstrates a much wider range of exposure levels. From an air quality perspective, the data reveals a concerning trend. Even though the medians are somewhat manageable, the extreme maximums ( $180$  for PM2.5 and  $250$  for PM10) are well above standard health guidelines in many jurisdictions. The significant gap between the median and the maximum values suggests that "average" air quality readings in this location may be misleading, as they fail to capture the severity of the frequent pollution peaks shown by the long upper whiskers. In conclusion, while PM2.5 shows more "stability" at lower levels, both pollutants exhibit extreme spikes that would necessitate public health interventions.



(a) Combined PM2.5 and PM10 concentration (b) concentration with Who thresholds

Figure 5. Combined PM2.5 and PM10 CDF

The provided visualization is a comparative boxplot designed to illustrate the distribution, central tendency, and variability of two critical air quality indicators: PM2.5 and PM10. The data is measured in micrograms per cubic meter ( $\mu\text{g}/\text{m}^3$ ) along the vertical axis, providing a clear window into the atmospheric conditions recorded in this dataset. Understanding the Visualization Tool To interpret this narrative, one must first understand the anatomy of a boxplot. Each plot consists of a central "box" representing the Interquartile Range (IQR), which contains the middle 50% of the data. The orange horizontal line within the box marks the median, or the 50th percentile. The vertical lines extending from the box, known as whiskers, represent the spread of the data from the minimum to the maximum values, excluding potential outliers. The PM2.5 plot represents "fine" particulate matter, which is particularly hazardous due to its ability to penetrate deep into the lungs. In this dataset, the median concentration sits relatively low, at approximately  $31 \mu\text{g}/\text{m}^3$ . The lower quartile (the bottom of the box) is positioned near 20, suggesting that for a significant portion of the time, air quality remains within a relatively moderate range. However, the most striking feature of the PM2.5 data is the upper whisker. It extends significantly upward, reaching a maximum value of roughly  $180 \mu\text{g}/\text{m}^3$ . This long "tail" indicates that while the typical day might have lower pollution levels, there are frequent or severe episodes where fine particulate matter spikes to dangerous levels, causing a highly skewed distribution.

### Detailed Breakdown of PM10

Turning to PM10, which includes larger particles like dust and pollen, we see a much broader and more intense profile. The median for PM10 is notably higher than that of PM2.5, hovering around the  $46 \mu\text{g}/\text{m}^3$ . The vertical size of the PM10 box is much larger than its counterpart, indicating a higher Interquartile Range. This tells us that PM10 levels are far more volatile and less predictable than PM2.5 levels. The data reaches a staggering peak at the top whisker, touching  $250 \mu\text{g}/\text{m}^3$ . This suggests that the environment being monitored is subject to significant influxes of larger particles, possibly driven by industrial activity, construction, or specific seasonal weather events.

When comparing the two, a clear pattern emerges: PM10 concentrations are consistently higher and more variable than PM2.5. The increased height of the PM10 box and its whiskers demonstrates a much wider range of exposure levels. From an air quality perspective, the data reveals a concerning trend. Even though the medians are somewhat manageable, the extreme maximums ( $180$  for PM2.5 and  $250$  for PM10) are well above standard health guidelines in many jurisdictions. The significant gap between the median and the maximum values suggests that "average" air quality readings in this location may be misleading, as they fail to capture the severity of the frequent pollution peaks shown by the long upper whiskers. In conclusion, while PM2.5 shows more "stability" at lower levels, both pollutants exhibit extreme spikes that would necessitate public health interventions.

This dual-pane visualization provides a comprehensive statistical and temporal analysis of particulate matter concentrations, specifically PM2.5 and PM10. By combining a **Cumulative Distribution Function (CDF)** with a **Time-Series plot**, the data illustrates not just the levels of pollution, but also the probability of exposure and the frequency of high-pollution events relative to health safety standards.

- **Statistical Profile: Cumulative Distribution Function (CDF)**

The left chart displays the CDF, which maps concentration ( $\mu\text{g}/\text{m}^3$ ) against its cumulative probability. This plot is essential for understanding the likelihood of encountering specific pollution levels.

The **PM2.5 curve (blue)** is positioned to the left of the **PM10 curve (orange)**, confirming that fine particles generally exist at lower concentrations than larger particles. A steep rise is observed in both curves between 0 and 50  $\mu\text{g}/\text{m}^3$ , indicating that for the majority of the time (roughly 60–70% probability), concentrations remain relatively low. However, the curves flatten out as they move to the right, representing the "long tail" of the data where rare but extreme pollution events occur. For instance, there is a 90% probability that PM2.5 remains below 140  $\mu\text{g}/\text{m}^3$  while for PM10, that same 90% threshold is not reached until roughly 200  $\mu\text{g}/\text{m}^3$ .

- **Temporal Analysis: Concentration over Time**

The right chart offers a 120-minute window into the actual behavior of these pollutants. The most striking feature of this graph is the presence of **two distinct peaks** occurring around the 40-minute and 80-minute marks.

- The First Peak:** PM10 surges to approximately 250  $\mu\text{g}/\text{m}^3$  while PM2.5 follows a similar pattern but peaks lower, at about 170  $\mu\text{g}/\text{m}^3$ .
- The Second Peak:** A slightly lower surge occurs at 80 minutes, with PM10 reaching 210  $\mu\text{g}/\text{m}^3$  and PM2.5 hitting 145  $\mu\text{g}/\text{m}^3$ .

These "twin peaks" suggest episodic pollution sources—perhaps passing traffic, industrial cycles, or specific localized activities. Between these spikes, the concentrations return to a "baseline" that fluctuates between 10 and 50  $\mu\text{g}/\text{m}^3$ .

## CONCLUSION

The comprehensive monitoring and analysis of air quality parameters presented in this study provide critical insights into the behavior of particulate matter (PM2.5 and PM10) within the observed environment. By synthesizing the results from the **Cumulative Distribution Function (CDF)**, **boxplot analysis**, and **time-series observations**, several fundamental conclusions can be drawn regarding atmospheric health and pollutant dynamics.

### Characterization of Pollutant Dynamics

The study confirms a strong correlation between **PM2.5** and **PM10** concentrations, with both pollutants exhibiting synchronized episodic surges. While the baseline air quality remains within manageable levels for a majority of the observation period (as evidenced by the steep initial gradient of the CDF curves), the environment is prone to extreme, short-lived pollution events. The identification of the "twin peaks" at the 40-minute and 80-minute intervals suggests that the primary threat to air quality in this area is not a persistent background haze, but rather **point-source emissions** or **periodic anthropogenic activities** (such as industrial cycles or traffic pulses).

### Public Health Implications and WHO Compliance

A critical finding of this research is the frequent and severe violation of **World Health Organization (WHO)** safety thresholds. Despite median concentrations appearing relatively stable, the peak events recorded concentrations exceeding safe limits by a factor of **10 to 15**.

- PM10** reached a maximum of 250  $\mu\text{g}/\text{m}^3$
- PM2.5** reached a maximum of 180  $\mu\text{g}/\text{m}^3$

These levels represent a significant acute respiratory risk. The data suggests that standard "daily average" reporting may obscure the true health hazards posed by these high-intensity, short-duration exposure windows.

### Summary of Findings and Recommendations

In summary, the air quality at the monitoring site is characterized by high volatility and significant episodic degradation. The research highlights that: **PM10** exhibits higher mass concentration and greater variability than **PM2.5**. The statistical "long tail" of the distribution indicates that extreme pollution events are a recurring feature of the local atmosphere rather than statistical anomalies. To improve local air quality, mitigation strategies must move beyond general emission reductions and focus on the **identification of the specific sources** responsible for the 40-minute and 80-minute surges. Implementing real-time alert systems based on the predictive patterns identified in the time-series data could significantly reduce public exposure during these peak intervals.

### REFERENCES

- Agbehadji, I. E., & Obagbuwa, I. C. (2025). Explainable Artificial Intelligence and Machine Learning for Air Pollution Risk Assessment and Respiratory Health Outcomes: A Systematic Review. In *Atmosphere* (Vol. 16, Issue 10, p. 1154). <https://doi.org/10.3390/atmos16101154>
- Alabdulkreem, E., Allafi, R., Arasi, M. A., Geetha, P., Nafie, F. M., Begum, A. S., Nallasivan, G., & Vivek, S. (2025). Innovative IoT and blockchain integration for real-time urban air quality monitoring and autonomous response system. *Sustainable Computing: Informatics and Systems*, 48, 101250. <https://doi.org/https://doi.org/10.1016/j.suscom.2025.101250>
- Armengol, J., Masip, V., Barrantes, A., Beltrami, G., Albiach, S., Rodriguez Rey, D., Guevara, M., Soret, A., Quiñones, E., & Kartsakli, E. (2025). *IoT- and AI-informed urban air quality models for vehicle pollution monitoring*. <https://doi.org/10.48550/arXiv.2511.00187>
- Azizah, D. N., Heranurweni, S., & Idris, L. O. M. (2025). Internet of Things Based Air Quality Monitoring System with Automatic Notification. *MALCOM: Indonesian Journal of Machine Learning and Computer Science*, 5(3 SE-), 776–787. <https://doi.org/10.57152/malcom.v5i3.1945>
- Bagkis, E., Hassani, A., Schneider, P., DeSouza, P., Shetty, S., Kassandros, T., Salamalikis, V., Castell, N., Karatzas, K., Ahlwat, A., & Khan, J. (2025). Evolving trends in application of low-cost air quality sensor networks: challenges and future directions. *Npj Climate and Atmospheric Science*, 8(1), 335. <https://doi.org/10.1038/s41612-025-01216-4>
- Chasapi, M.-A., Moustiris, K., Fameli, K.-M., & Spyropoulos, G. (2025). The Application of an Empirical Method for the Estimation of Vehicles' Contribution to Air Pollution in an Urban Environment: A Case Study in Athens, Greece. In *Air* (Vol. 3, Issue 2, p. 14). <https://doi.org/10.3390/air3020014>
- Chen, J., González, Ó., O'Connor, D., Tallon, L., & Pilla, F. (2025). Assessment of IoT low-cost sensor networks for long-term outdoor and indoor air quality monitoring: a case study in Dublin. *Atmospheric Pollution Research*, 16, 102651. <https://doi.org/10.1016/j.apr.2025.102651>
- Gabriel, M. F., Marques, G., Filipe, D., Felgueiras, F., Cardoso, J. P., Azeredo, J., Kazdaridis, G., Symeonidis, P., Keranidis, S., Conradie, P., Azevedo, I., & Anagnostopoulos, F. (2024). Implementation of an IoT architecture for promoting healthy air quality in 84 homes of families with children. *Building and Environment*, 266, 112040. <https://doi.org/https://doi.org/10.1016/j.buildenv.2024.112040>
- Garcia, A., Saez, Y., Harris, I., Huang, X., & Collado, E. (2025). Advancements in air quality monitoring: a systematic review of IoT-based air quality monitoring and AI technologies. *Artificial Intelligence Review*, 58(9), 275. <https://doi.org/10.1007/s10462-025-11277-9>
- Gueye, A., Drame, M., & Niang, S. A. A. (2024). A low-cost IoT-based real-time pollution monitoring system using ESP8266 NodeMCU. *Measurement and Control*, 58, 1337–1345. <https://doi.org/10.1177/00202940241306690>
- Hassan, A. K., Saraya, M. S., Ali-Eldin, A. M. T., & Abdelsalam, M. M. (2024). Low-Cost IoT Air Quality Monitoring Station Using Cloud Platform and Blockchain Technology. In *Applied Sciences* (Vol. 14, Issue 13, p. 5774). <https://doi.org/10.3390/app14135774>
- Hwang, S., Park, J., Chu, Y.-T., & Choi, J. (2026). A GNN-based interpolation method for enhancing air pollution prediction based on Internet of Things (IoT) data. *Atmospheric Environment*, 371, 121835. <https://doi.org/https://doi.org/10.1016/j.atmosenv.2026.121835>
- Jang, B.-J., Park, N., & Jung, I. (2025). IoT Sensing-Based High-Density Monitoring of Urban Roadside Particulate Matter (PM10 and PM2.5). *Applied Sciences*, 15, 11608. <https://doi.org/10.3390/app152111608>
- Karmoude, M., Munhungewarwa, B., Chiraira, I., Mckenzie, R., Kong, J., Smith, B., Ayana, G., Njara, N., Mathaha, T., Kumar, M., & Mellado, B. (2025). Machine learning for air quality prediction and data analysis: Review on recent advancements, challenges, and outlooks. *Science of The Total Environment*, 1002, 180593.

- <https://doi.org/https://doi.org/10.1016/j.scitotenv.2025.180593>
- Kumaran, G., & Mohan, S. (2026). A Review on Air Pollution Prediction Using Artificial Intelligence. *IEEE Access, PP*, 1. <https://doi.org/10.1109/ACCESS.2026.3664880>
- Li, Y., Guo, J., Sun, S., Li, J., Wang, S., & Zhang, C. (2022). Air quality forecasting with artificial intelligence techniques: A scientometric and content analysis. *Environmental Modelling & Software*, 149, 105329. <https://doi.org/https://doi.org/10.1016/j.envsoft.2022.105329>
- Lopes, S. I., Orłowski, C., Branco, P. T. B. S., Karatzas, K., Villena, G., Saffell, J., Marques, G., Sousa, S. I. V., Lenartz, F., Bergmans, B., Bigi, A., Pflanzner, T., & Ródenas García, M. (2025). Low-Cost Sensor Systems and IoT Technologies for Indoor Air Quality Monitoring: Instrumentation, Models, Implementation, and Perspectives for Validation. In *Sensors* (Vol. 25, Issue 24, p. 7567). <https://doi.org/10.3390/s25247567>
- Luangwilai, T., Kunno, J., Manomaipiboon, B., Ruamtawee, W., & Ong-Artborirak, P. (2025). Risk Perception and Self-Monitoring of Particulate Matter 2.5 (PM 2.5) Associated with Anxiety Among General Population in Urban Thailand. In *Urban Science* (Vol. 9, Issue 7, p. 256). <https://doi.org/10.3390/urbansci9070256>
- Maulidi, A., Sambodho, K., Dinariyana, A. A. B., & Syafruddin, M. (2025). IoT Based Early Monitoring System for Air Quality Assessment. *IOP Conference Series: Earth and Environmental Science*, 1473(1), 12010. <https://doi.org/10.1088/1755-1315/1473/1/012010>
- O'Regan, A. C., Grythe, H., Schneider, P., & Nyhan, M. M. (2026). Integrating Low-Cost Sensors with Dispersion Modelling for High-Resolution Insights into Urban Air Quality. *Environment International*, 209, 110157. <https://doi.org/https://doi.org/10.1016/j.envint.2026.110157>
- Otanasap, N., Chalernsuk, C., & Tadsuan, S. (2024). An AIoT based Air Quality Monitoring System for Real-time PM2.5 Prediction in Urban Environments. *ASEAN Journal of Scientific and Technological Reports*, 28, e255168. <https://doi.org/10.55164/ajstr.v28i1.255168>
- Peixe, J., & Marques, G. (2024). Low-cost IoT-enabled indoor air quality monitoring systems: A systematic review. *Journal of Ambient Intelligence and Smart Environments*, 16, 1–14. <https://doi.org/10.3233/AIS-220577>
- Relvas, H., Lopes, D., & Armengol, J. M. (2025). Empowering communities: Advancements in air quality monitoring and citizen engagement. *Urban Climate*, 60, 102344. <https://doi.org/https://doi.org/10.1016/j.uclim.2025.102344>
- Wu, C., Wang, R., Lu, S., Tian, J., Yin, L., Wang, L., & Zheng, W. (2025). Time-Series Data-Driven PM2.5 Forecasting: From Theoretical Framework to Empirical Analysis. In *Atmosphere* (Vol. 16, Issue 3, p. 292). <https://doi.org/10.3390/atmos16030292>